

# The Mass Spectrum of Black Holes in Close Binary Systems

A. I. Bogomazov<sup>1</sup>, M. K. Abubekrov<sup>2</sup>, and V. M. Lipunov<sup>1,2</sup>

<sup>1</sup>*Moscow State University, Moscow, Russia*

<sup>2</sup>*Sternberg Astronomical Institute, Universitetskii pr. 13, Moscow, Russia*

Received January 20, 2005; in final form, February 17, 2005

**Abstract**—We present the results of population syntheses obtained using our “scenario machine.” The mass spectra of black holes in X-ray binary systems before and after the stage of accretion from an optical companion are obtained for various evolutionary scenarios. The results of the model computations are compared to observational data. The observational data are used to estimate the fraction of a pre-supernova’s mass that collapses into a black hole. This model can explain the formation of low-mass ( $2\text{--}4 M_{\odot}$ ) black holes in binary systems with optical companions. We show that the number of low-mass black holes in the Galaxy is sufficiently high for them to be detected. The population-synthesis results suggest that the vast majority of low-mass black holes are formed via the accretion-induced collapse of neutron stars. The percentage of low-mass black holes in binary systems that form due to accretion-induced collapse is 2–15% of the total number of black holes in binaries, depending on the evolutionary scenario. © 2005 Pleiades Publishing, Inc.

## 1. INTRODUCTION

Currently, about a thousand X-ray sources have been detected in the Milky Way and nearby galaxies [1, 2], most of which are close binary systems in which an optical component supplies matter to a neutron star or black hole. However, mass estimates have been derived for only  $\sim 30$  neutron stars and  $\sim 20$  black holes. This number is not sufficient to enable firm conclusions about the properties of the mass spectrum of relativistic objects.

Thus, the mass spectrum of compact objects is not well known due to poor statistics and insufficient accuracy in the estimated masses of neutron stars and black holes. In addition, the lack of compact objects with masses between  $2$  and  $6 M_{\odot}$  in the observed mass distribution for neutron stars and black holes is striking. This gap is especially surprising in the light of new data on the masses of the CO cores of Wolf–Rayet stars at the end of their evolution [3], which are continuously distributed over a wide range,  $M_{\text{CO}} = (1\text{--}2)\text{--}(20\text{--}44) M_{\odot}$ . Since it is thought that Wolf–Rayet stars are progenitors of relativistic objects [4–6], such a large difference between the final masses of the CO cores of Wolf–Rayet stars and the masses of the relativistic objects that they are thought to produce requires an explanation. For this reason, with the aim of determining the possible masses of black holes and the shape of the mass spectrum of compact objects before and after accretion of matter from the optical companion, we carried out population syntheses using the “scenario machine” described in [7].

Accretion onto neutron stars and estimates of the mass accumulated on their surfaces have been analyzed in detail in [8]. The aim of the present paper is to model the mass spectrum of black holes in binary systems with optical components (BH + opt).

## 2. OBSERVATIONAL DATA

As we noted above, masses have been estimated for more than 30 neutron stars and about 20 black

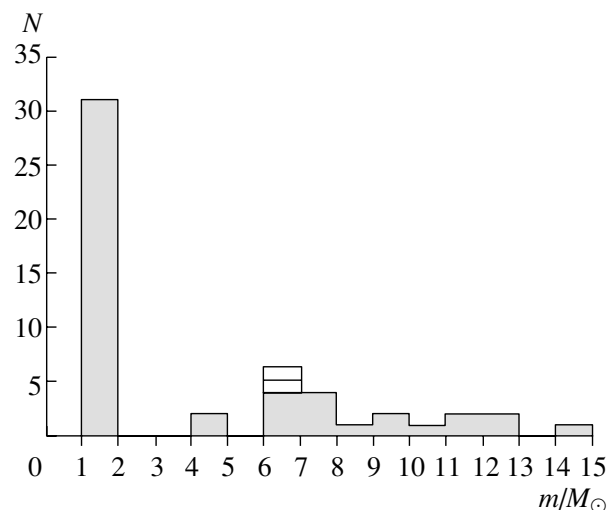


**Fig. 1.** Observed mass distribution of compact objects. The open rectangles show the masses of black holes derived from microlensing experiments [9].

**Table 1.** Masses of black holes in binary systems

Name	$i$ , deg	$f(M)$ , $M_{\odot}$	$m_{BH}$ , $M_{\odot}$	$m_{opt}$ , $M_{\odot}$	References
Cyg X-1	31–44	$0.2580 \pm 0.0007$	$11.05 \pm 2.55$	$22.0 \pm 0.51$	[10]
LMC X-1	$\sim 63$	$0.14 \pm 0.05$	$7 \pm 3$	$22 \pm 4$	[2, 11]
LMC X-3	$67 \pm 3$	$2.29 \pm 0.32$	5.94–9.17	3–8	[12–14]
SS 433	90	$7.7 \pm 1.1$	$11 \pm 5$	$19 \pm 7$	[15]
A0620-00	$40.75 \pm 3$	$2.72 \pm 0.06$	$11.0 \pm 1.9$	$0.68 \pm 0.18$	[16]
V404 Cyg	54–64	$5.819 \pm 0.003$	$10.65 \pm 1.95$	$0.64 \pm 0.12$	[17]
GRS 1124-683	$54 \pm 1.5$	$3.01 \pm 0.15$	$6.95 \pm 0.6$	$0.75 \pm 0.05$	[18, 19]
GRS 1915+105	$70 \pm 2$	$9.5 \pm 3.0$	$14 \pm 4$	$1.2 \pm 0.2$	[2, 11]
GS 2000+25	$64 \pm 1.3$	$5.01 \pm 0.12$	7.15–7.78	0.25–0.41	[11]
GRO J0422+32	$45 \pm 2$	$1.19 \pm 0.02$	$3.97 \pm 0.95$	$0.46 \pm 0.31$	[35]
GRO J1655-40	$70.2 \pm 1.9$	$2.73 \pm 0.09$	$6.3 \pm 0.5$	$2.4 \pm 0.4$	[20]
H 1705-250	$70 \pm 10$	$4.86 \pm 0.13$	4.9–7.9	$0.26 \pm 0.42$	[21, 22]
4U 1543-47	$20.7 \pm 1.5$	$0.25 \pm 0.01$	8.45–10.39	2.0–2.5	[11]
GRS 1009-45	$\sim 78$	$3.17 \pm 0.12$	$4.4^{+0.34}_{-0.76}$	$0.6^{+0.05}_{-0.10}$	[34]
SAX J1819.3-25	$75 \pm 2$	$3.13 \pm 0.13$	6.82–7.42	2.35–3.34	[11]
XTE J1118+480	$81 \pm 2$	$6.1 \pm 0.3$	6.0–7.7	0.09–0.5	[23]
XTE J1550-564	67–77.4	$6.86 \pm 0.71$	$9.41^{+1.35}_{-1.05}$	$< 0.79$	[24]
XTE J1859+226	–	$7.4 \pm 1.1$	7.6–12.0	–	[25]
GX 339-4	–	$5.8 \pm 0.5$	–	–	[26]
XTE 1650-500*	–	–	$\sim 8.2$	–	[27]

\* Mass estimate obtained from high-frequency quasi-periodic oscillations in the X-ray.

holes. The mass distribution of these relativistic objects is shown in Fig. 1. The black-hole masses are listed in Tables 1 and 2. The neutron-star masses presented in Fig. 1 are already given in [8], and we do not list them here.

Figure 1 shows that this distribution is bimodal [3, 28, 29]. The masses of the neutron stars are confined to a narrow range, with the average mass being  $1.35 \pm 0.15 M_{\odot}$ . The black-hole masses are distributed over a relatively wide range:  $m_{BH} = 4\text{--}15 M_{\odot}$ . The average black-hole mass is  $6.64 \pm 0.77 M_{\odot}$ .

No candidate black holes with masses of  $2\text{--}4 M_{\odot}$  have been discovered. Only the central masses of the compact components of the close binary systems Vela X-1, 4U 1700–37, and J0751+1807 fall in this range. The compact objects in these systems are neutron stars with masses close to  $\sim 2 M_{\odot}$ . As recent studies have shown [30–32], the estimated masses

of the compact objects in Vela X-1, 4U 1700–37, and J0751+1807 are not firm enough to be confident that massive neutron stars ( $m_{NS} > 1.8 M_{\odot}$ ) are present in these systems. For this reason, we placed the masses of the neutron stars in Vela X-1, 4U 1700–37, and J0751+1807 in the  $1\text{--}2 M_{\odot}$  bin in Fig. 1. The method used to estimate the masses of the neutron stars in these binaries and results based on these estimates are considered in detail in [33].

**Table 2.** Masses of black holes based on observations of microlensing

Name	$m_{BH}$ , $M_{\odot}$	References
MACHO-96-BLG-5	$6^{+10}_{-3}$	[9]
MACHO-98-BLG-6	$6^{+7}_{-3}$	[9]

The central mass estimates of the compact components in the X-ray binaries GRS 1009-45 and GRO J0422+32 are in the range  $4\text{--}6 M_{\odot}$  (Fig. 1), making the relativistic objects in these binary systems candidate low-mass black holes. According to [34], the mass of the GRS 1009-45 black hole is  $4.4^{+0.34}_{-0.76} M_{\odot}$ ; the mass of the GRO J0422+32 black hole is  $3.97 \pm 0.95 M_{\odot}$  [35]. Note that this latter estimate is not entirely firm. In particular, according to [36], the mass of this black hole exceeds  $9 M_{\odot}$ . We have adopted the more recent mass estimate obtained in [35].

The central mass estimates for the remaining candidate black holes exceed  $6 M_{\odot}$  (Table 1). The mass distribution for the candidate black holes with  $m_{BH} \geq 6 M_{\odot}$  has a broad peak at  $6\text{--}8 M_{\odot}$  and a uniform tail extending to  $14 M_{\odot}$ .

We are considering predominantly mass estimates for compact objects obtained using dynamical methods (i.e., from observations of the radial-velocity curve of the optical companion), which are most accurate and reliable. The masses of the candidate black holes MACHO-96-BLG-5 and MACHO-98-BLG-6 derived from microlensing observations are listed in Table 2. Due to their lower accuracy, these two mass estimates are shown as unfilled entries in Fig. 1.

Due to the meagre statistics, it is not possible to determine the shape of the mass spectrum for the observed black holes with confidence (Fig. 1). However, we can use the existing black-hole mass estimates to find the ratio of the numbers of low- and high-mass black holes in binary systems:

$$R = N(m_{BH} \leq m_{BH}^{\min}) / N(m_{BH} > m_{BH}^{\min}). \quad (1)$$

Based on the mass estimates listed in Table 1, we took  $m_{BH}^{\min}$  to be  $\sim 4 M_{\odot}$ . Accordingly, we took black holes with masses lower than  $\sim 4 M_{\odot}$  to be “low-mass” and black holes with masses greater than  $\sim 4 M_{\odot}$  to be “high-mass” black holes. The observational estimates of the black-hole masses in Table 1 yield a ratio of the numbers of low- and high-mass black holes in binary systems  $R_{obs} \lesssim 1/10$ . The parameter  $R$  served as a criterion of the adequacy of the various models in terms of the observational statistics of the masses of black holes in close binaries.

Another such criterion was that an adequate model should have at least one Cyg X-1-like system per Galaxy (per  $\sim 10^{11}$  stars). Following [37], we suppose that Cyg X-1 is not a statistical outlier, and that there may be several such systems in the Galaxy. Support for this hypothesis is provided by the existence of similar candidate systems in the Large Magellanic Cloud: LMC X-1 and LMC X-3. In the model computations, we considered a binary to be a

Cyg X-1-like system if it contains a massive optical star ( $m_{opt} \geq 10 M_{\odot}$ ) close to Roche-lobe overflow and a massive black hole ( $m_{BH} > 4 M_{\odot}$ ) that is accreting from a disk (for more details see [38]).

The last important requirement of the population-synthesis calculations was the virtual absence of black holes in pairs with radio pulsars (BH + PSR systems). To exclude observational selection effects, we used the ratio of the numbers of BH + PSR systems and of all radio pulsars to evaluate this criterion  $N(\text{BH} + \text{PSR})/N(\text{PSR})$ . According to the observational data, there are no radio pulsars in binaries with black holes among the  $\sim 1500$  detected radio pulsars. Thus, in the model Galaxy, the ratio  $N(\text{BH} + \text{PSR})/N(\text{PSR})$  should not exceed  $1/1500$ .

The above criteria based on observational information enabled us to restrict in advance the model parameters used in the “scenario machine.”

### 3. POPULATION SYNTHESIS

#### *General Description of the Model*

With the aim of determining the shape of the black-hole mass spectrum before and after the accretion stage, we carried out population-synthesis computations for  $10^6$  binary systems under various assumptions about their evolution using the “scenario machine.” The computations assumed a Salpeter initial mass function for the binary components:

$$f(m) = m^{-2.35}. \quad (2)$$

The initial component masses were varied from  $10 M_{\odot}$  to  $120 M_{\odot}$ . Population-synthesis computations were carried out for two distributions of the initial component-mass ratio  $f(q) = q^{\alpha_q}$ : uniform ( $\alpha_q = 0$ ) and quadratic ( $\alpha_q = 2$ ), where  $q = m_2/m_1$ . We considered masses of the secondary  $m_2$  and primary  $m_1$  such that  $m_1 > m_2$ . The distribution of the binaries over the initial component separation  $f(a)$  was taken to obey the function

$$f(a) = 1/a \quad (3)$$

(see [39] for more details). The initial semi-major axis of the orbit could have any value in the range  $(10\text{--}10^6) R_{\odot}$ .

We selected from the computation results only black holes with optical companions (BH + opt). Among the many parameters of the BH + opt systems that form, we are interested in the masses  $m_{BH}$  and lifetimes of the black holes. Since black holes undergo an accretion stage during their evolution, we considered the black-hole mass spectrum in BH + opt systems both before and after this stage.

We assumed that the strengths of the anisotropic kicks that the nascent black holes receive in supernova explosions have a Maxwellian distribution:

$$f(v) \sim \frac{v^2}{v_0^2} e^{-\frac{v^2}{v_0^2}}, \quad (4)$$

with all directions having equal probability. However, the magnitude of the kick after the supernova  $v_0$  remains an important but poorly studied parameter. The results of the population synthesis are very sensitive to  $v_0$ . A sharp increase of  $v_0$  results in a sharp decrease of the number of systems with relativistic companions. The  $v_0$  value for neutron stars is 100–180 km/s [40], but the typical value of  $v_0$  for black holes formed via collapse is not currently known.

Taking the typical anisotropic kick velocity for neutron stars to be  $v_0 = 180$  km/s [40] and assuming that the magnitude of the kick acquired by the neutron star during the collapse depends on the mass of the ejected envelope, we specified the value of  $v_0$  for black holes using the relation

$$v_0 = 180 \frac{m_{preSN} - m_{BH}}{m_{BH}} \text{ km/s}, \quad (5)$$

where  $m_{preSN}$  is the mass of the presupernova and  $m_{BH}$  the mass of the nascent black hole.

The mass-loss rate of the optical star  $\dot{m}$  is also a relatively poorly studied parameter. For this reason, we carried out model computations for three mass-loss scenarios during the evolution of a star, which we label A, B, and C. We also carried out a computation for the Woosley model of stellar evolution [41, 42]. The scenario based on the Woosley model is labeled W.

#### *Evolutionary Scenario A*

The mass-loss rate in the main-sequence (MS) stage is described by the classical formula of de Jager [43]:

$$\dot{m} \sim L/V_\infty, \quad (6)$$

where  $L$  is the star's luminosity and  $V_\infty$  the terminal velocity of the stellar wind.

For giants, we used the larger of the values given by (6) and by the expression of Lamers [44]:

$$\dot{m} \sim L^{1.42} R^{0.61} / m^{0.99}, \quad (7)$$

where  $R$  and  $m$  are the radius and mass of the star.

For the red supergiant stage, we used the larger of the values given by (6) and by the wind model of Kudritzki and Reimers [45]:

$$\dot{m} \sim LR/m. \quad (8)$$

The change of the star's mass  $\Delta m$  during a single stage in the model with type-A wind does not exceed  $0.1(m - m_{core})$ , where  $m$  is the mass of the star at the beginning of this stage and  $m_{core}$  is the mass of the stellar core. The mass loss in the Wolf–Rayet stage was parameterized as  $0.1 m_{WR}$ , where  $m_{WR}$  is the maximum stellar mass in this stage. We used the core masses computed in [46–48] to calculate the parameters of the type-A wind.

In scenario A, the mass lost by a star did not exceed 30% of its initial mass  $m_{opt}$ .

#### *Evolutionary Scenario B*

In scenario B, we used the results of the evolutionary computations of [49], which indicate that a massive star loses up to  $\sim 90\%$  of its initial mass in the main-sequence, supergiant, and Wolf–Rayet stages via its stellar wind. Therefore, the presupernova mass in scenario B was  $\sim 8\text{--}10 M_\odot$ , essentially independent of the mass of the parent star.

#### *Evolutionary Scenario C*

In scenario C, the mass-loss rate in the main-sequence, supergiant, and Wolf–Rayet stages was based on the computations of Vanbeveren [50], which reproduce the observed distribution of Galactic Wolf–Rayet stars and the stellar-wind mass loss by massive stars accurately. The computations made use of the relation

$$\Delta m = (m - m_{core}), \quad (9)$$

where the stellar core mass  $m_{core}$  is defined as

$$m_{core} = \begin{cases} 1.62m_{opt}^{0.83} & \text{for MS stars,} \\ 10^{-3.051+4.21 \log m_{opt}-0.93(\log m_{opt})^2} & \text{for supergiants,} \\ 0.83m_{WR}^{0.36} & \text{for Wolf–Rayet stars with } m_{WR} < 2.5 M_\odot, \\ 1.3 + 0.65(m_{WR} - 2.4) & \text{for Wolf–Rayet stars with } m_{WR} > 2.5 M_\odot, \\ m_{core} = 3.03m_{opt}^{0.342} & \text{for Wolf–Rayet stars with } m_{max} > 2.5 M_\odot. \end{cases} \quad (10)$$

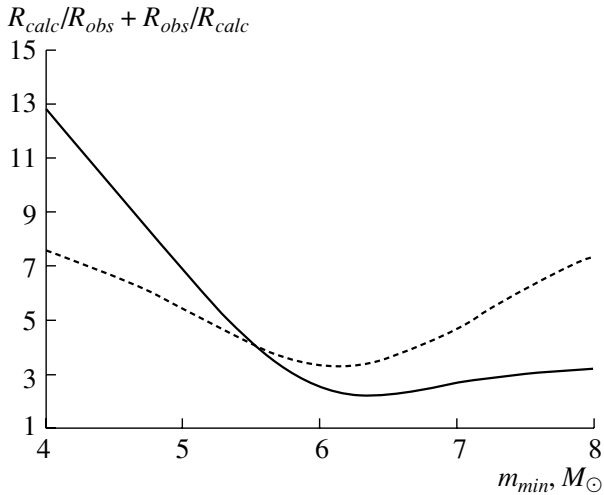


**Fig. 2.** Dependence of  $R_{calc}/R_{obs} + R_{obs}/R_{calc}$  on  $m_{min}$  in scenarios A (solid curve) and C (dashed curve); see the text for more details. The parameter  $k_{BH} = 0.5$ .

Evolutionary scenario C has moderate mass loss, and a mass-loss rate that is lower than in scenario B, but higher than in scenario A. For example, in scenario C, a star with an initial mass of  $m_{opt} > 15 M_{\odot}$  can lose up to 30% of its initial mass in the main-sequence, giant, and supergiant stages. We applied scenario A for the computations of mass loss by lower-mass stars with  $m_{opt} < 15 M_{\odot}$ . A high mass loss in the Wolf–Rayet stage is typical of scenario C, with the Wolf–Rayet star losing up to  $\sim 50\%$  of its initial mass.

#### Evolutionary Scenario W

Evolutionary scenario W is based on the evolutionary diagram for stars of various masses published by Woosley [41, Fig. 16], which represents the relationship between the mass of the relativistic remnant and the initial mass of the star. We carried out population-synthesis computations for two models with W-type stellar winds, which we label Wb and Wc. In models Wb and Wc, the mass-loss rates were computed as in scenario B and scenario C, respectively. The use of these models to calculate the wind rate in a scenario based on Woosley’s diagram [41, Fig. 16] is justified by the fact that scenarios B and C are based on the same numerical expressions for the mass-loss rates from [49–51] that were used by Woosley in his work (see [7] for more details).

#### 4. THE MINIMUM BLACK-HOLE MASS

One of the important parameters of the population syntheses is the minimum mass of the black holes formed in supernovae,  $m_{min}$ . Since this parameter

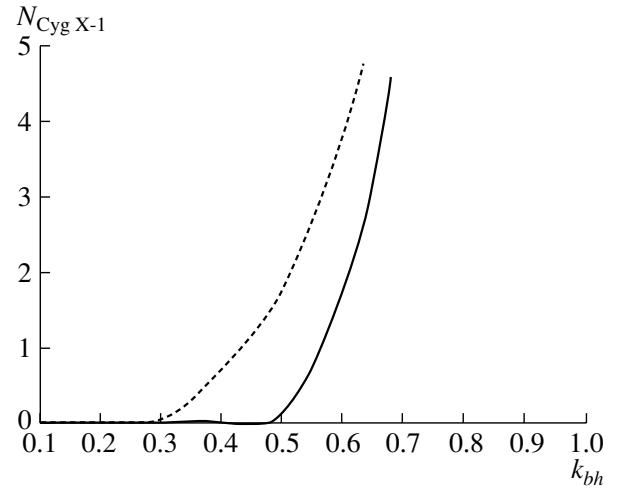


**Fig. 3.** Dependence of the number of Cyg X-1-like systems in the Galaxy on  $k_{BH} = 0.5$  in model A (for  $\alpha_q = 0$ , dashed curve) and model C (for  $\alpha_q = 2$ , solid curve).

is not known precisely, we carried out population-synthesis computations for several values of  $m_{min}$  in the range  $2.5–10 M_{\odot}$ . We found that the maximum of the black-hole mass spectrum corresponds to  $m_{min}$ . We can see from the observational data (Table 1 and Fig. 1) that the maximum of the black-hole mass spectrum is in the range  $6–8 M_{\odot}$ , i.e.,  $m_{min}$  should be close to  $7 M_{\odot}$ .

Additional evidence that  $m_{min}$  is close to  $7 M_{\odot}$  is provided by special model computations carried out for this purpose. In these computations, we calculated the parameter  $R_{calc}$  [the ratio of the numbers of low- and high-mass black holes; see Eq. (1)] for  $m_{min} = 2, 3, 4, \dots, 10 M_{\odot}$ . The computations were carried out for scenarios A and C, and assumed that half of the presupernova mass  $m_{preSN}$  collapses into a black hole (with mass  $m_{BH}$ ). Figures 2a,b show the dependence of  $R_{calc}/R_{obs} + R_{obs}/R_{calc}$  on  $m_{min}$  in evolutionary scenarios A and C. Recall that we assumed that the observed ratio of the numbers of low- and high-mass black holes  $R_{obs} = 1/10$  (Table 1). In both cases (Figs. 2a and 2b), the minimum of  $R_{calc}/R_{obs} + R_{obs}/R_{calc}$ , which is related to  $R_{calc}/R_{obs}$ , corresponds to  $m_{min} \simeq 6–6.5 M_{\odot}$ .

Given these results, in the subsequent model computations, we set the minimum mass of a black hole formed in a supernova to  $m_{min} = 7 M_{\odot}$ . This does not preclude the formation of black holes with masses below  $7 M_{\odot}$ . For example, in all the evolutionary scenarios (A, B, C, and W) we allowed for the accretion-induced collapse of a neutron star into a black hole if the mass of the neutron star grew to the Oppenheimer–Volkoff limit, which we took to be  $2 M_{\odot}$ .

### 5. THE MASS FRACTION OF PRESUPERNOVA THAT COLLAPSE INSIDE THE EVENT HORIZON

An important parameter that enters the population-synthesis algorithm is the fraction of presupernovae with masses of  $m_{preSN}$  that collapse into black holes with masses of  $m_{BH}$ . In scenarios A, B, and C, the mass of the black hole  $m_{BH}$  produced by the explosion of a presupernova with mass  $m_{preSN}$  was computed as

$$m_{BH} = k_{BH} m_{preSN}, \quad (11)$$

where the constant coefficient  $k_{BH}$  is the fraction of the presupernova mass that collapses inside the event horizon. In scenario W,  $k_{BH}$  was taken to be variable, and to have a value determined by the dependence of the mass of the compact remnant on the initial mass of the optical star [41, Fig. 16].

The best-fit value of  $k_{BH}$  in scenarios A, B, and C was searched for. Population syntheses were carried out for each value of  $k_{BH}$  in the range from 0.1 to 1.0 with steps of 0.1. The other population-synthesis parameters in this set of calculations were held fixed. When varying the value of  $k_{BH}$ , we monitored the number of Galactic Cyg X-1-like systems produced in the computations. The results are presented in Fig. 3. Following [37, 38], we assumed that Cyg X-1-like systems are not statistical outliers, and are always present in the Galaxy. We assume that approximately one such system should exist in the Galaxy at any given time. This criterion yielded  $k_{BH}$  values of 0.43 for scenario A (Fig. 3) and 0.57 for scenario C (Fig. 3). In scenario B, no Cyg X-1-type systems were produced for any of the  $k_{BH}$  values in the range 0.1–1.0. For this reason, we rejected scenario B as being unrealistic. Further runs of the population synthesis code were carried out for scenarios A, C, and W.

### 6. BLACK-HOLE MASS SPECTRA IN MODEL A

For each scenario, a population synthesis was carried out for  $10^6$  initial binaries. For models A and C, we assumed that the initial distribution of the component-mass ratios in the binaries was flat ( $\alpha_q = 0$ ). The results obtained for a quadratic distribution ( $\alpha_q = 2$ ) did not satisfy the observational criteria.

The spectrum of initial black-hole masses obtained for scenario A, shown in Fig. 4a, is clearly bimodal. Most of the black-hole masses are concentrated in the range 7–12  $M_\odot$ , although there are also low-mass black holes ( $m_{BH} = 2\text{--}3 M_\odot$ ) present in

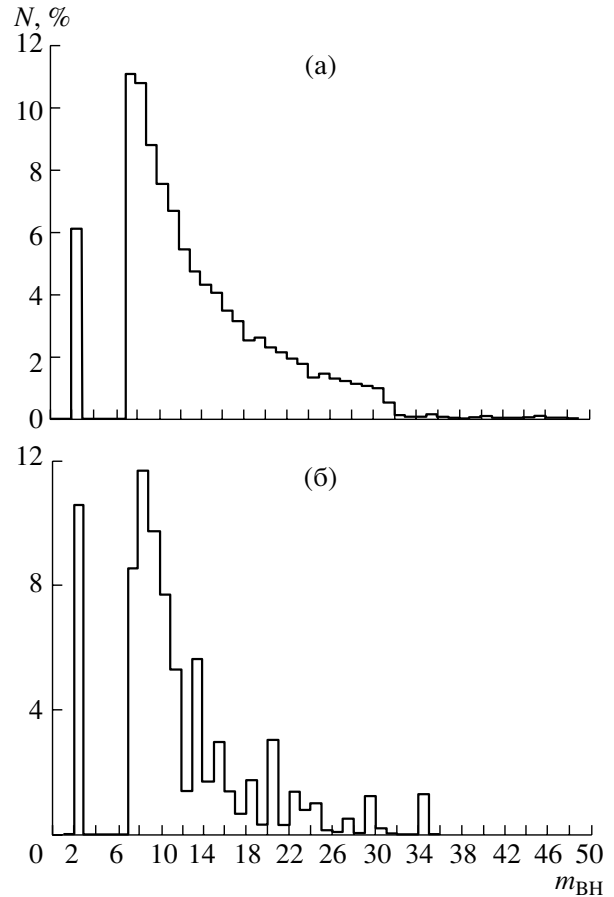


**Fig. 4.** (a) Initial model mass spectrum for black holes in BH + opt binaries for scenario A ( $\alpha_q = 0$  and  $k_{BH} = 0.43$ ; see the text for more details). (b) The same spectrum after taking into account observational selection effect due to the difference in the lifetimes of optical stars.

the spectrum. These low-mass black holes are produced by collapses of neutron stars whose masses grow to the Oppenheimer–Volkoff limit [8].

The overwhelming majority of black holes ( $\sim 99.99\%$  of the total number) do not increase their mass in the course of their evolution due to the accretion of matter from their optical companion. Only a negligible fraction ( $\sim 0.01\%$  of the total number) increase their mass by  $\Delta m \simeq 1 M_\odot$ . For this reason, the shape of the black-hole mass spectrum in model A is the same before and after the accretion stage (therefore, we do not show the latter here). Figure 4b shows the black-hole mass spectrum in the final stage of the evolution of the optical component, corrected for selection effects due to differences in the lifetimes of different binaries in the BH + opt stage. These were taken into account using the formula

$$N(m_k) = \sum_{j=0}^{n_k} t_j / \sum_{i=0}^N t_i, \quad (12)$$

**Table 3.** Observational parameters derived via the population syntheses for evolutionary scenarios A, C, and W

Observational parameter	Observational data*	A	C	Wc
Number of Cyg X-1-type systems in the Galaxy	1	$\approx 1$	$\approx 1$	$\approx 1$
$\frac{N(\text{BH} + \text{PSR})}{N(\text{PSR})}$	$< \frac{1}{1500}$	$\approx \frac{1}{1500}$	$\approx \frac{1.3}{1500}$	$\approx \frac{1.5}{1500}$
$R = \frac{N(m_{\text{BH}} < 4.0M_{\odot})}{N(m_{\text{BH}} \geq 4.0M_{\odot})}$	$\sim 0.1$	$\approx 0.15$	$\approx 0.03$	$\approx 0.03$

\* See the text for more details.

where  $N(m_k)$  is the number of black holes with masses in the range  $m_k + dm_k$  ( $m_k = 1, 2, 3, 4 \dots M_{\odot}$ , and  $dm_k = 1 M_{\odot}$ ),  $n_k$  the number of black holes in the bin for mass  $m_k$ ,  $t_j$  the lifetime of a binary with a black-hole of mass in the interval  $m_k + dm_k$ ,  $N$  the total number of model tracks ( $N = 10^6$ ), and  $t_i$  the lifetime of a binary with a black hole. We can see that, after correcting for differences in the stellar lifetimes in the BH + opt stage, the bimodal structure of the mass spectrum

becomes even more pronounced (Fig. 4). Thus, the population-synthesis results for scenario A suggest that the masses of the vast majority of black holes should be confined to  $8\text{--}15 M_{\odot}$ . However, the model computations confirm the possible formation of low-mass ( $m_{\text{BH}} = 2\text{--}4 M_{\odot}$ ) black holes in binary systems. The number of binaries with low-mass black holes is fairly high: there should exist one low-mass ( $m_{\text{BH}} \leq 4 M_{\odot}$ ) black-hole system for every  $\sim 7$  binaries with high-mass ( $m_{\text{BH}} > 4 M_{\odot}$ ) black holes. In scenario A, low-mass black holes are produced only by accretion-induced collapse, and they comprise  $\sim 15\%$  of the total number of black holes in binaries. The numerical criteria characterizing the consistency of model A with the observational data are presented in Table 3.

## 7. BLACK-HOLE MASS SPECTRA IN MODEL C

Recall that the value of  $k_{\text{BH}}$  in evolutionary scenario C was set to 0.57, and that the minimum black-hole mass was set to  $7 M_{\odot}$ . The shape of the initial black-hole mass spectrum is shown in Fig. 5a. In contrast to scenario A, the scenario C spectrum has three peaks (Fig. 5a). Black holes with masses  $2\text{--}4 M_{\odot}$  are formed only via the accretion-induced collapse of neutron stars. In contrast to scenario A, the fraction of low-mass black holes in scenario C is  $\sim 5\%$  of the total number of all black holes that are formed in binary systems.

Figure 5a shows that, in scenario C, most ( $\sim 54.5\%$ ) black holes have masses of  $7\text{--}9 M_{\odot}$  at the time of formation of the BH + opt system. All black holes with masses of  $7\text{--}9 M_{\odot}$  descend from Wolf-Rayet stars. Black holes with masses of  $10\text{--}12 M_{\odot}$  comprise  $\sim 40.5\%$  of the total number of black holes, and are produced by collapses of presupernovae that avoided the Wolf-Rayet stage.

Due to the high mass loss in the main-sequence, supergiant, and Wolf-Rayet stages (up to 50% of the initial mass), no very massive black holes are produced in scenario C. Thus, the maximum mass of black holes in this scenario is  $12 M_{\odot}$  (Fig. 5).

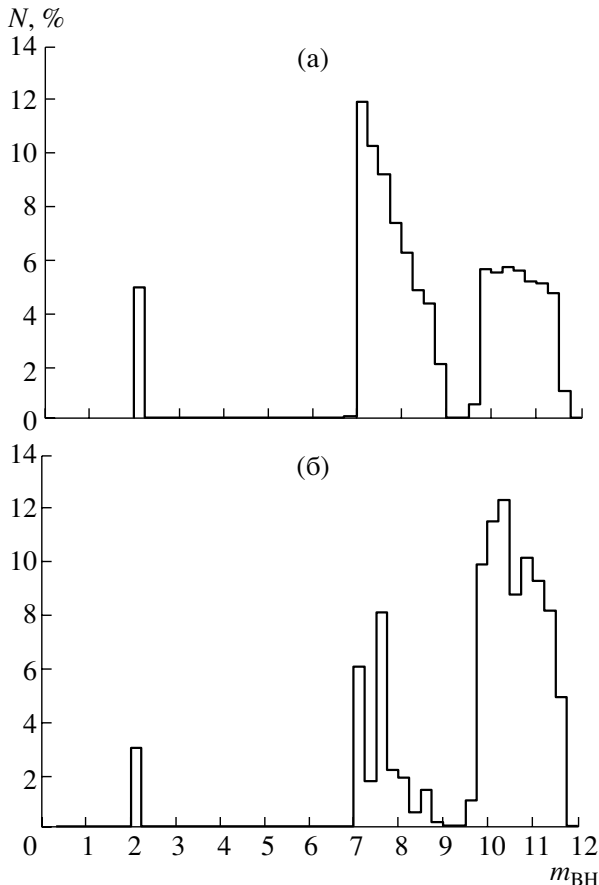


**Fig. 5.** Same as Fig. 4 for scenario C ( $\alpha_q = 0$  and  $k_{\text{BH}} = 0.57$ ).

As in scenario A, only  $\sim 0.01\%$  of black holes increase their mass by  $\Delta M \simeq 1 M_\odot$  during the evolution of the binary system. The masses of most black holes remain unchanged or increased by only  $\Delta m \simeq 0.01 M_\odot$  due to accretion. For this reason we do not show the mass spectrum of the post-accretion black holes. Figure 5b shows the black-hole mass spectrum at the end of the evolution of the optical component, corrected for differences in the lifetimes of binaries in the BH + opt stage using formula (12) with  $dm_k = 0.25 M_\odot$ .

Selection effects due to differences in the lifetimes of binaries in the BH + opt stage had an appreciable influence on the initial black-hole mass distribution (Figs. 5a, 5b). In scenario C, black holes with masses exceeding  $12 M_\odot$  should not be observed, and a considerable fraction of black holes ( $\sim 76\%$ ) should have masses  $\sim 10\text{--}12 M_\odot$ . Black holes with masses  $\sim 7\text{--}9 M_\odot$  comprise  $\sim 21\%$  of the total number of observed black holes. Note that there are few low-mass black holes in the “observed” distribution of black holes produced in scenario C ( $\sim 3\%$  of the total number of black holes). In the total sample, the ratio of the numbers of low- and high-mass black holes is  $R \simeq 0.03$ . The numerical criteria characterizing the consistency of model C with the observational data are presented in Table 3.

## 8. BLACK-HOLE MASS SPECTRUM IN SCENARIO W

Scenario Wb did not satisfy the observational criteria: not a single Cyg X-1-like system was produced in the model Galaxy ( $10^{11}$  stars). For this reason, we considered scenario Wb to be unrealistic, and did not analyze it further. Scenario Wc fitted the required observational criteria sufficiently well (Table 3), and we, accordingly, carried out population-synthesis computations for this scenario.

As we noted above, scenario Wc is based on the relation of [41] between the mass of the optical star  $m_{opt}$  and the mass of the compact remnant, as well as a dependence of the mass loss on  $m_{opt}$  similar to that in scenario C. The maximum black-hole mass in the model of Woosley [41, Fig. 16] did not exceed  $\sim 11 M_\odot$ . This model assumed that black holes are produced by stars with initial masses greater than  $20.7 M_\odot$ . The initial distribution of the component-mass ratios was taken to be quadratic:  $\alpha_q = 2$ . The hypothesis of a flat initial mass-ratio distribution was rejected based on the observational criteria: the number of Cyg X-1-like systems was far greater than one per model Galaxy.

The initial black-hole mass spectrum obtained for evolutionary scenario Wc is shown in Fig. 6a. The masses of  $\sim 10\%$  of the produced black holes are in the

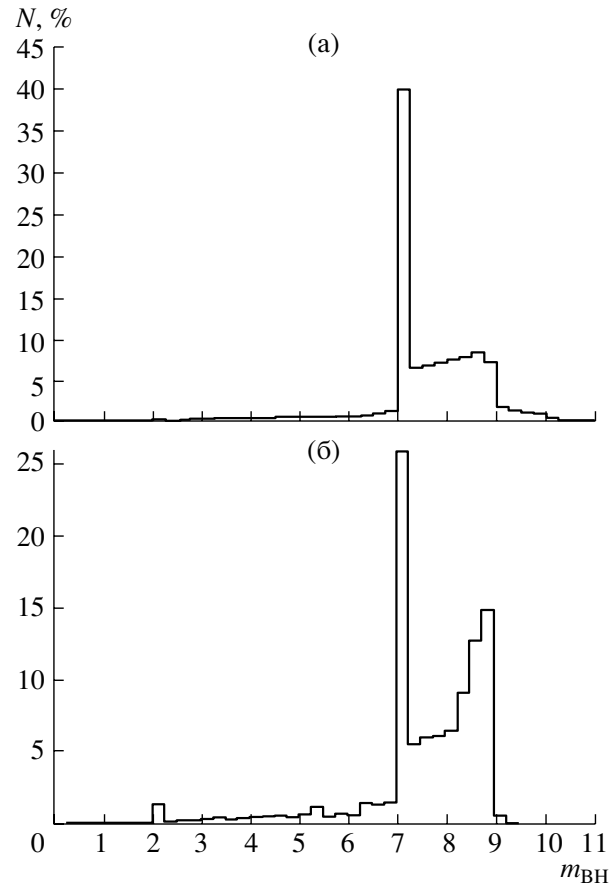


Fig. 6. Same as Fig. 4 for scenario Wc with  $\alpha_q = 2$  and with  $k_{BH}$  values that depend on the initial mass of the star.

range  $2\text{--}7 M_\odot$ , while about  $45\%$  of the black holes have masses of  $7.1\text{--}7.5 M_\odot$ . The fraction of black holes with masses exceeding  $7.5 M_\odot$  is also  $\sim 45\%$ .

The peak of the histogram at  $\sim 7 M_\odot$  is due to the nature of the relation between the mass of the optical star  $m_{opt}$  and the mass of the black hole produced by this star [41, Fig. 16]. Stars with masses of  $20.7\text{--}27 M_\odot$  produced low-mass black holes with  $m_{BH} \simeq 2\text{--}6 M_\odot$ . Due to the low-mass of the nascent black holes and the considerable mass loss in the supernova explosions, the vast majority of binaries could not remain bound after the collapse. This explains the deficit of black holes with masses of  $m_{BH} \simeq 2\text{--}6 M_\odot$ .

According to the evolutionary scheme of [41], optical stars with masses of  $27\text{--}84 M_\odot$  are the progenitors of  $\sim 7 M_\odot$  black holes. This feature of the scheme results in the peak in the initial black-hole mass distribution (Fig. 6a). Black holes with masses  $m_{BH} > 7.5 M_\odot$  are produced by optical stars with initial masses of  $\gtrsim 84 M_\odot$ . We do not present the post-accretion black-hole mass spectrum, since it is very similar to the initial mass spectrum.

Figure 6b shows the black-hole mass spectrum after correcting for differences in the lifetimes of the BH + opt systems using formula (12) with  $dm_k = 0.25 M_\odot$ . We can see that this selection effect strongly influences the mass distribution of the black holes. The group of low-mass black holes ( $m_{BH} < 4 M_\odot$ ) in BH + opt systems becomes much more prominent: such black holes comprise  $\sim 3\%$  of all “observed” black holes in scenario W (see Fig. 6b). About 2% of the total number of low-mass black holes in binary systems are produced by accretion-induced collapses of neutron stars in scenario Wc (Fig. 6). At the same time, all the low-mass ( $m_{BH} \leq 4 M_\odot$ ) black holes in scenarios A and C were produced by accretion-induced collapses of neutron stars.

The maximum of the black-hole mass distribution remained at  $\sim 7 M_\odot$ , but the total number around this peak was reduced to  $\sim 25\%$  of the total number of black holes in BH + opt binaries. The fraction of black holes with masses  $m_{BH} \simeq 7.5\text{--}9 M_\odot$  in BH + opt binaries increased to  $\sim 60\%$  (Fig. 6b). Note that the maximum mass of an “observed” black hole in a pair with an optical companion in scenario W is  $m_{BH} \simeq 9 M_\odot$ . The numerical criteria characterizing the consistency of the population-synthesis results for model Wc with the observational data are presented in Table 3.

## 9. CONCLUSION

The formation of BH + opt binaries with low-mass black holes ( $m_{BH} = 2\text{--}4 M_\odot$ ) in all three evolutionary scenarios (A, C, and W) is one of the most important results of our computations. The population-synthesis results indicate that  $\sim (3\text{--})15\%$  of the total number of black holes in binary systems with optical companions in scenarios A, C, and W are low-mass black holes. In other words, according to our computations, the number of low-mass black holes ( $m_{BH} = 2\text{--}4 M_\odot$ ) in binaries with optical companions is sufficiently high to enable their detection in the near future. It is not ruled out that the objects GRS 1009-45 and GRO J0422+32 (Table 1), which contain compact objects with estimated masses  $m_{BH} = 2\text{--}4 M_\odot$  (within current levels of accuracy), are black holes produced by accretion-induced collapse.

According to the population-synthesis results, accretion plays a negligible role in the formation of the mass spectrum of black holes in BH + opt systems. On the other hand, selection effects related to the lifetimes of binary systems considerably distort the intrinsic shape of the mass spectrum (Figs. 4–6).

The poor statistics of black-hole mass estimates and limited accuracy of these estimates prevent us from identifying one of the scenarios as being “correct.” With the current accuracy of the observed

black-hole mass spectrum, all three scenarios (A, C, and W) satisfy both the observational criteria (Table 1) and the observed mass spectrum (Fig. 1).

The population-synthesis results for scenarios A and W suggest that the masses of the vast majority of black holes that will be discovered in the future will be in the range  $7\text{--}9 M_\odot$ . If scenario C is the most realistic, the masses of most “new” black holes will be  $10\text{--}12 M_\odot$ . According to scenario A, black holes with masses up to  $\sim 50 M_\odot$  may be present in binary systems.

To conclude, we note the recent discovery of the compact object 2S 0921-630, with an estimated mass of  $1.9\text{--}2.9 M_\odot$  [53]. The nature of this object is not yet known, but, given our population-synthesis results, we cannot rule out the possibility that 2S 0921-630 is a low-mass black hole. Recall that, according to our computations, 3–15% of all the black holes in binaries may be low-mass black holes.

We stress that, according to the population-synthesis computations, the overwhelming majority of low-mass black holes ( $2\text{--}4 M_\odot$ ) are formed via accretion-induced collapses of neutron stars. Therefore, we expect that the masses of a high fraction of low-mass black holes should be very close to the Oppenheimer–Volkoff limit ( $\sim 2.5\text{--}3 M_\odot$ ).

## ACKNOWLEDGMENTS

The authors thank A.M. Cherepashchuk for providing references to the observational data. The authors are very grateful to S.B. Popov, A.G. Kuranov, M.E. Prokhorov, I.E. Panchenko, and K.A. Postnov for valuable remarks and advice. This study was supported by the program “Leading Scientific Schools of Russia” (NSh 388.2003.2) and the Russian Foundation for Basic Research (project no. 04-02-16411).

## REFERENCES

1. A. M. Cherepashchuk, *Usp. Fiz. Nauk* **166**, 809 (1996) [*Phys. Usp.* **39**, 759 (1996)].
2. A. M. Cherepashchuk, *Usp. Fiz. Nauk* **173**, 345 (2003) [*Phys. Usp.* **46**, 335 (2003)].
3. A. M. Cherepashchuk, *Astron. Zh.* **78**, 145 (2001) [*Astron. Rep.* **45**, 120 (2001)].
4. A. V. Tutukov and L. R. Yungel’son, *Nauchni Inform. Astrosovet Akad. Nauk SSSR* **27**, 58 (1973).
5. E. P. J. van den Heuvel and J. Heise, *Nature Phys. Sci.* **239**, 67 (1972).
6. L. R. Yungel’son and A. M. Cherepashchuk, *Astron. Zh.* **80**, 419 (2003) [*Astron. Rep.* **47**, 386 (2003)].
7. V. M. Lipunov, K. A. Postnov, and M. E. Prokhorov, *Astrophysics and Space Physics Reviews*, Ed. by R. A. Sunyaev (Harwood, Amsterdam, 1996), Vol. 9.

8. A. I. Bogomazov, M. K. Abubekеров, V. M. Lipunov, and A. M. Cherepashchuk, *Astron. Zh.* **82**, 331 (2005) [*Astron. Rep.* **49**, 295 (2005)].
9. D. P. Bennett, A. C. Becker, J. L. Quinn, *et al.*, *Astrophys. J.* **579**, 639 (2002).
10. M. K. Abubekеров, E. A. Antokhina, and A. M. Cherepashchuk, *Astron. Zh.* **81**, 606 (2004) [*Astron. Rep.* **48**, 550 (2004)].
11. J. A. Orosz, in *IAU Symposium No. 212: A Massive Star Odyssey: From Main Sequence to Supernova*, Ed. by K. van der Hucht, A. Herrero, and E. Cesar (Astron. Soc. Pac., San Francisco, 2003), p. 365; astro-ph/0209041.
12. M. van der Klis, M. Clausen, K. Jensen, *et al.*, *Astron. Astrophys.* **151**, 322 (1985).
13. A. P. Cowley, D. Crampton, J. B. Hutchings, *et al.*, *Astrophys. J.* **272**, 118 (1983).
14. L. Kuiper, M. van der Klis, and J. van Paradijs, *Astron. Astrophys.* **203**, 79 (1988).
15. D. R. Gies, W. Huang, and M. V. McSwain, *Astrophys. J.* **578**, L67 (2002).
16. D. M. Gelino, T. E. Harrison, and J. A. Orosz, *Astron. J.* **122**, 2668 (2001).
17. A. M. Cherepashchuk, N. V. Borisov, M. K. Abubekеров, *et al.*, *Astron. Zh.* **81**, 1119 (2004) [*Astron. Rep.* **48**, 1019 (2004)].
18. D. M. Gelino, T. E. Harrison, and B. J. McNamara, *Astron. J.* **122**, 971 (2001).
19. I. Baraffe, G. Chabrier, F. Allard, and P. H. Hauschildt, *Astron. Astrophys.* **337**, 403 (1998).
20. D. M. Greene, C. D. Bailyn, and J. A. Orosz, *Astrophys. J.* **554**, 1290 (2001).
21. R. A. Remillard, J. A. Orosz, J. E. McClintock, and J. E. C. D. Bailyn, *Astrophys. J.* **459**, 226 (1996).
22. E. T. Harlaftis, D. Steeghs, K. Horne, and J. E. A. V. Filippenko, *Astron. J.* **144**, 1170 (1997).
23. R. M. Wagner, C. B. Foltz, T. Shahbaz, *et al.*, *Astrophys. J.* **556**, 42 (2001).
24. J. A. Orosz, P. J. Groot, M. van der Klis, *et al.*, *Astrophys. J.* **568**, 845 (2002).
25. A. V. Filippenko and R. Chornock, *IAU Circ.*, No. 7644, 2 (2001).
26. R. I. Hynes, D. Steeghs, J. Casares, *et al.*, *Astrophys. J.* **583**, L95 (2003).
27. J. Homan, M. Klein-Wolt, S. Rossi, *et al.*, *Astrophys. J.* **586**, 1262 (2003).
28. C. D. Bailyn, R. K. Jain, P. Coppi, and J. A. Orosz, *Astrophys. J.* **499**, 367 (1998).
29. A. M. Cherepashchuk, in *Modern Problems in Stellar Evolution*, Ed. by D. S. Wiebe (GEOS, Moscow, 1998), p. 198.
30. M. K. Abubekеров, E. A. Antokhina, and A. M. Cherepashchuk, *Astron. Zh.* **81**, 108 (2004) [*Astron. Rep.* **48**, 89 (2004)].
31. M. K. Abubekеров, *Astron. Zh.* **81**, 714 (2004) [*Astron. Rep.* **48**, 649 (2004)].
32. D. J. Nice, E. M. Splaver, and I. H. Stairs, astro-ph/0411207.
33. M. K. Abubekеров and A. M. Cherepashchuk, *Astrofiz.* (2005) (in press).
34. A. V. Filippenko, D. C. Leonard, T. Matheson, W. Li, E. S. Moran, and A. G. Riess, *Publ. Astron. Soc. Pac.* **111**, 969 (1999).
35. D. M. Gelino and T. E. Harrison, *Astrophys. J.* **599**, 1254 (2003).
36. A. M. Cherepashchuk, *Space Sci. Rev.* **93**, 473 (2000).
37. J. van Paradijs and J. E. McClintock, *X-ray Binaries*, Ed. by W. H. G. Lewin, J. van Paradijs, and E. P. J. van den Heuvel (Cambridge Univ. Press, Cambridge, 1993).
38. V. M. Lipunov, A. I. Bogomazov, and M. K. Abubekеров, *Mon. Not. R. Astron. Soc.* (2005) (in press).
39. Z. T. Kraicheva, E. I. Popova, A. V. Tutukov, and L. R. Yungel'son, *Astron. Zh.* **56**, 520 (1979) [*Sov. Astron.* **23**, 290 (1979)].
40. V. M. Lipunov, K. A. Postnov, and M. E. Prokhorov, *Mon. Not. R. Astron. Soc.* **288**, 245 (1997).
41. S. E. Woosley, A. Heger, and T. A. Weaver, *Rev. Mod. Phys.* **74**, 1015 (2002).
42. A. Heger *et al.*, astro-ph/0211062.
43. C. Jager, *The Brightest Stars* (Dordrecht, Reidel, 1980).
44. H. J. G. L. M. Lamers, *Astrophys. J.* **245**, 593 (1981).
45. B. P. Kudritzki and D. Reimers, *Astron. Astrophys.* **70**, 227 (1978).
46. V. I. Varshavskii and A. V. Tutukov, *Astron. Zh.* **52**, 227 (1975) [*Sov. Astron.* **19**, 142 (1975)].
47. I. Iben, Jr. and A. V. Tutukov, *Astrophys. J.* **58**, 661 (1985).
48. I. Iben, Jr. and A. V. Tutukov, *Astrophys. J.* **313**, 727 (1981).
49. G. Schaller, D. Schaerer, G. Meynet, and A. Maeder, *Astron. Astrophys.*, Suppl. Ser. **96**, 269 (1992).
50. D. Vanbeveren, *New Astron.* **3**, 443 (1998).
51. H. Nieuwenhuijzen and C. de Jager, *Astron. Astrophys.* **231**, 134 (1990).
52. W. R. Hamman and L. Koesterke, *Astron. Astrophys.* **335**, 1003 (1998).
53. P. G. Jonker, D. Steegh, G. Nelemans, and M. van der Klis, *Mon. Not. R. Astron. Soc.* **356**, 621 (2005).

*Translated by L. Yungel'son*